

Cronos Titin Is Expressed in Human Cardiomyocytes and Necessary for Normal Sarcomere Function

BACKGROUND: The giant sarcomere protein titin is important in both heart health and disease. Mutations in the gene encoding for titin (*TTN*) are the leading known cause of familial dilated cardiomyopathy. The uneven distribution of these mutations within *TTN* motivated us to seek a more complete understanding of this gene and the isoforms it encodes in cardiomyocyte (CM) sarcomere formation and function.

METHODS: To investigate the function of titin in human CMs, we used CRISPR/Cas9 to generate homozygous truncations in the Z disk (*TTN-Z^{-/-}*) and A-band (*TTN-A^{-/-}*) regions of the *TTN* gene in human induced pluripotent stem cells. The resulting CMs were characterized with immunostaining, engineered heart tissue mechanical measurements, and single-cell force and calcium measurements.

RESULTS: After differentiation, we were surprised to find that despite the more upstream mutation, *TTN-Z^{-/-}*-CMs had sarcomeres and visibly contracted, whereas *TTN-A^{-/-}*-CMs did not. We hypothesized that sarcomere formation was caused by the expression of a recently discovered isoform of titin, Cronos, which initiates downstream of the truncation in *TTN-Z^{-/-}*-CMs. Using a custom Cronos antibody, we demonstrate that this isoform is expressed and integrated into myofibrils in human CMs. *TTN-Z^{-/-}*-CMs exclusively express Cronos titin, but these cells produce lower contractile force and have perturbed myofibril bundling compared with controls expressing both full-length and Cronos titin. Cronos titin is highly expressed in human fetal cardiac tissue, and when knocked out in human induced pluripotent stem cell derived CMs, these cells exhibit reduced contractile force and myofibrillar disarray despite the presence of full-length titin.

CONCLUSIONS: We demonstrate that Cronos titin is expressed in developing human CMs and is able to support partial sarcomere formation in the absence of full-length titin. Furthermore, Cronos titin is necessary for proper sarcomere function in human induced pluripotent stem cell derived CMs. Additional investigation is necessary to understand the molecular mechanisms of this novel isoform and how it contributes to human cardiac disease.

Rebecca J. Zaunbrecher, PhD
Ashley N. Abel, BS
Kevin Beussman, MS
Andrea Leonard, PhD
Marion von Frieling-Salewsky, BS
Paul A. Fields, PhD
Lil Pabon, PhD
Hans Reinecke, PhD
Xiulan Yang, MD, PhD
Jesse Macadangdang, PhD
Deok-Ho Kim, PhD
Wolfgang A. Linke, PhD
Nathan J. Sniadecki, PhD
Michael Regnier, PhD
Charles E. Murry, MD, PhD

Key Words: cardiomyopathy
■ induced pluripotent stem cells
■ myocytes, cardiac ■ sarcomere assembly

Sources of Funding, see page 1658

© 2019 American Heart Association, Inc.

<https://www.ahajournals.org/journal/circ>

Clinical Perspective

What Is New?

- Our studies using genetically engineered human induced pluripotent stem cell derived cardiomyocytes experimentally confirm that the gene encoding the giant sarcomere protein titin (*TTN*) includes an internal promoter and start site.
- This internal start site encodes for the isoform Cronos, which we demonstrate is able to support some sarcomere formation in human induced pluripotent stem cell derived cardiomyocytes.
- To the best of our knowledge, this is the first study to experimentally demonstrate that Cronos is expressed in fetal and adult cardiac tissue and is necessary for proper human cardiomyocyte function.

What Are the Clinical Implications?

- Truncating mutations in *TTN* are the leading known cause of familial dilated cardiomyopathy.
- Cronos titin is a previously unstudied form of titin that we show is necessary for normal human cardiomyocyte function and could be contributing to these titinopathies.
- Truncating mutations in *TTN* are most often found in the regions of the gene included in Cronos titin, warranting further investigation into its role in dilated cardiomyopathy pathogenesis.

The giant sarcomere protein titin has a number of important roles in cardiac muscle, where it extends an entire half-sarcomere length from the Z disk to the M line and interacts with both the thick and thin filaments.¹ Titin is a modular protein with 4 main regions: The N-terminus of titin is anchored to the Z disk of the sarcomere through interactions with T-cap and α -actinin,^{2,3} as well as with the noncontractile cytoskeleton.^{4,5} The spring-like I band of titin provides the majority of passive tension in cardiomyocytes (CMs),^{6,7} whereas the rigid A-band region interacts with the thick filament and has been proposed to act as a molecular ruler that establishes the patterning of myosin.^{8–12} The C-terminus of titin is anchored in the M line by myomesin and contains a kinase domain, which is activated by stretch to promote sarcomere protein turnover.^{13,14} Titin is known to be required for the proper function of sarcomeres. However, conflicting evidence exists about the necessity of titin in sarcomerogenesis. In cultured primary cardiomyocytes, titin is difficult to specifically and completely knock down because of its genetic complexity and large size.¹⁵ In vivo studies of early sarcomerogenesis are challenging because of the embryonic lethality associated with homozygous truncating mutations of titin.^{16,17} Because of these roadblocks, a major unanswered question is whether titin is crucial

for sarcomere formation or only necessary for proper function once sarcomeres are fully formed.

In addition to its important role in healthy CMs, heterozygous truncating mutations in the gene encoding for titin (*TTN*) are the leading known cause of familial dilated cardiomyopathy (DCM), accounting for $\approx 25\%$ of cases.^{18–22} Despite the high prevalence of titin-truncating mutations in patients with DCM, the pathogenicity of these mutations in the general population is not straightforward. Approximately 0.5% to 0.7% of healthy control populations carry truncating mutations in *TTN*, a rate at least twice that of the total prevalence of nonischemic DCM.^{17,22–25} Because of the high prevalence of apparently nondeleterious titin-truncating mutations, there has been significant interest in determining whether the pathogenicity of variants can be predicted on the basis of their location within *TTN*. One hypothesis to predict the disease-causing potential of variants is that mutations occurring in constitutively expressed exons are more pathogenic than those in variably spliced exons.^{24,26} Although this hypothesis explains the high odds ratio of 32 for mutations in the A-band region of titin, the majority of which are constitutively spliced in, it does not account for the lower pathogenicity of truncation mutations in other constitutively expressed regions of *TTN* such as the Z disk, which has an odds ratio of 19.5.¹⁷ These differences suggest that there may be other aspects of the gene architecture of *TTN* that have not yet been characterized that contribute to disparate clinical results of truncating mutations.

To elucidate the role of titin during sarcomere development and to better understand *TTN* expression, we have taken the approach of genetically engineering homozygous truncating mutations into human induced pluripotent stem cells (hiPSCs) and studying their function after differentiation into CMs (hiPSC-CMs). Genetic engineering in vitro allows the dissection of titin-specific effects at early developmental stages that would not be possible with animal models. Understanding titin expression and function in hiPSC-CMs is especially important because these cells are often used to study heterozygous titin-truncating mutations for disease modeling.^{26–28} Because heterozygous truncating mutations in the A-band region of titin are more pathogenic than those in the Z disk region, we introduced homozygous truncating mutations in each of these locations to determine whether they caused different phenotypes. A previous study of hiPSC-CMs carrying a homozygous A-band titin truncation found that the cells lacked sarcomeres,²⁶ and because of the embryonic lethality of homozygous titin truncations in both the Z disk and A band in animal models,^{16,17} we hypothesized that both mutations would prevent sarcomere formation in hiPSC-CMs. Although A-band truncations blocked sarcomere formation, we were surprised to find that CMs with Z disk truncations formed sarcomeres and visibly contracted, albeit much

more weakly than wild type (WT) hiPSC-CMs. Sarcomere assembly in Z disk truncations was associated with the expression of Cronos, a newly described titin isoform with a start site downstream of the truncating mutation in these cells.²⁹ In contrast, this isoform is absent (or truncated) in A-band truncations, where sarcomere formation is not observed. We further show that Cronos is highly expressed in developing human hearts and may be involved in sarcomerogenesis. When Cronos is specifically knocked out in hiPSC-CMs, the cells produce lower contractile force and develop sarcomeric disarray despite the presence of full-length titin. We conclude that Cronos titin is expressed in human CMs and is necessary for normal sarcomere formation and function.

METHODS

The data, analytical methods, and study materials will be made available to other researchers for purposes of reproducing the results or replicating the procedure.

CRISPR/Cas9 Targeting of *TTN* in hiPSCs

Single guide RNAs targeting *TTN* exons 2 and 326 and the Cronos-specific region were designed with the online CRISPR design tool (crispr.mit.edu; single guide RNA sequences are listed in [Table 1 in the online-only Data Supplement](#)) using the hg19 assembly *TTN* sequence on the University of California Santa Cruz Genome Browser³⁰ and predicted Cronos start site from Zou et al²⁹ and used as outlined in the [Methods in the online-only Data Supplement](#). For all cell lines generated, colonies with homozygous or compound heterozygous mutations causing premature stop codons were also screened for mutations in the top 5 genes predicted to be most susceptible to off-target effects (details in [Methods in the online-only Data Supplement](#)). Mutant cell lines were cryopreserved and karyotyped (Diagnostic Cytogenetics Inc, Seattle, WA).

Cardiac Differentiation

WT and mutated WTC11 hiPSCs were differentiated into CMs using a previously described monolayer protocol³¹ (details in [Methods in the online-only Data Supplement](#)) and maintained in RPMI media (Gibco) supplemented with 2% B-27 with insulin (Life Technologies) and 1% penicillin/streptomycin (Invitrogen). For single-cell force, calcium, and morphology measurements and live-cell imaging, CMs were purified with lactate selection by replating cells 14 to 18 days after the start of differentiation and feeding with DMEM without glucose (Gibco) supplemented with 4 $\mu\text{mol/L}$ sodium lactate (Sigma-Aldrich) on days 18 to 22 after differentiation.³² Cells used for calcium and morphology measurements were cultured in media containing 10 $\mu\text{mol/L}$ cytosine β -D-arabino-furanoside (Sigma-Aldrich) for 2 days after replating as single CMs.

Engineered Heart Tissues

Engineered heart tissues (EHTs) were cast 23 to 32 days after the start of differentiation with the use of a previously described fibrin scaffold system.³³ Each EHT was seeded with 4×10^5 hiPSC-CMs and 4×10^4 HS27a bone marrow stromal

cells (ATCC) resuspended in 100 μL fibrin solution and cast between 1 rigid and 1 flexible post made from silicone rubber (polydimethylsiloxane, Sylgard 184). EHTs were maintained in RPMI media supplemented with 2% B-27 with insulin, 1% penicillin/streptomycin, and 5 mg/mL aminocaproic acid (Sigma-Aldrich), which was changed every 2 to 3 days. After 3 weeks in culture, the deflection of the flexible posts during 1.5-Hz pacing was tracked by light microscopy. Force was calculated by multiplying the flexible post stiffness ($k=0.95 \mu\text{N}/\mu\text{m}$) by the measured post deflection, and the twitch kinetics were obtained from the force profiles.

Live-Cell Imaging

hiPSC-CMs were transduced with ELF1a-mCherry- α -actinin lentivirus ranging from days 23 to 35 after differentiation. Viral medium was changed 24 hours after transduction. Cells recovered for 6 days with regular maintenance and then were replated for imaging as described in the [Methods in the online-only Data Supplement](#).

Statistical Analysis

For assays with 2 groups, Student *t* tests were performed in Excel. For assays with >2 groups, 1-way ANOVAs were performed in MATLAB with the *anova1* function, and if the returned *P* value was <0.01, a Tukey post hoc analysis was performed with the *multcompare* function. Adjusted *P* values were computed with the Benjamini and Hochberg method.

Institutional Review Board

The studies for this articles did not include any human or animal studies. Thus, Institutional Review Board approval was not required.

RESULTS

Human iPSC Line Generation, Differentiation, and Titin Expression

To investigate the role of titin truncation mutations in CM differentiation and sarcomerogenesis, the CRISPR/Cas9 system was used to introduce truncation mutations via nonhomologous end joining into the WTC11 hiPSC line.³⁴ Mutations were targeted in exon 2 (in the Z disk domain; *TTN-Z^{-/-}*) and exon 326 (in the A-band region; *TTN-A^{-/-}*) of *TTN* using 2 different guide RNAs and generating 2 separate clonal lines for each locus (Figure 1A). Both of these exons are constitutively expressed in CMs but not in pluripotent cells.²⁶ Single-cell colonies were expanded and screened for homozygous mutations that introduce a stop codon and are thus expected to cause truncations. All mutant cell lines had normal karyotypes and normal colony morphology and growth (Figure 1 in the [online-only Data Supplement](#)). After induction with activin A, BMP4, and small-molecule Wnt modulators, all lines differentiated into high-purity populations of CMs as measured by flow cytometry after staining for cardiac troponin T

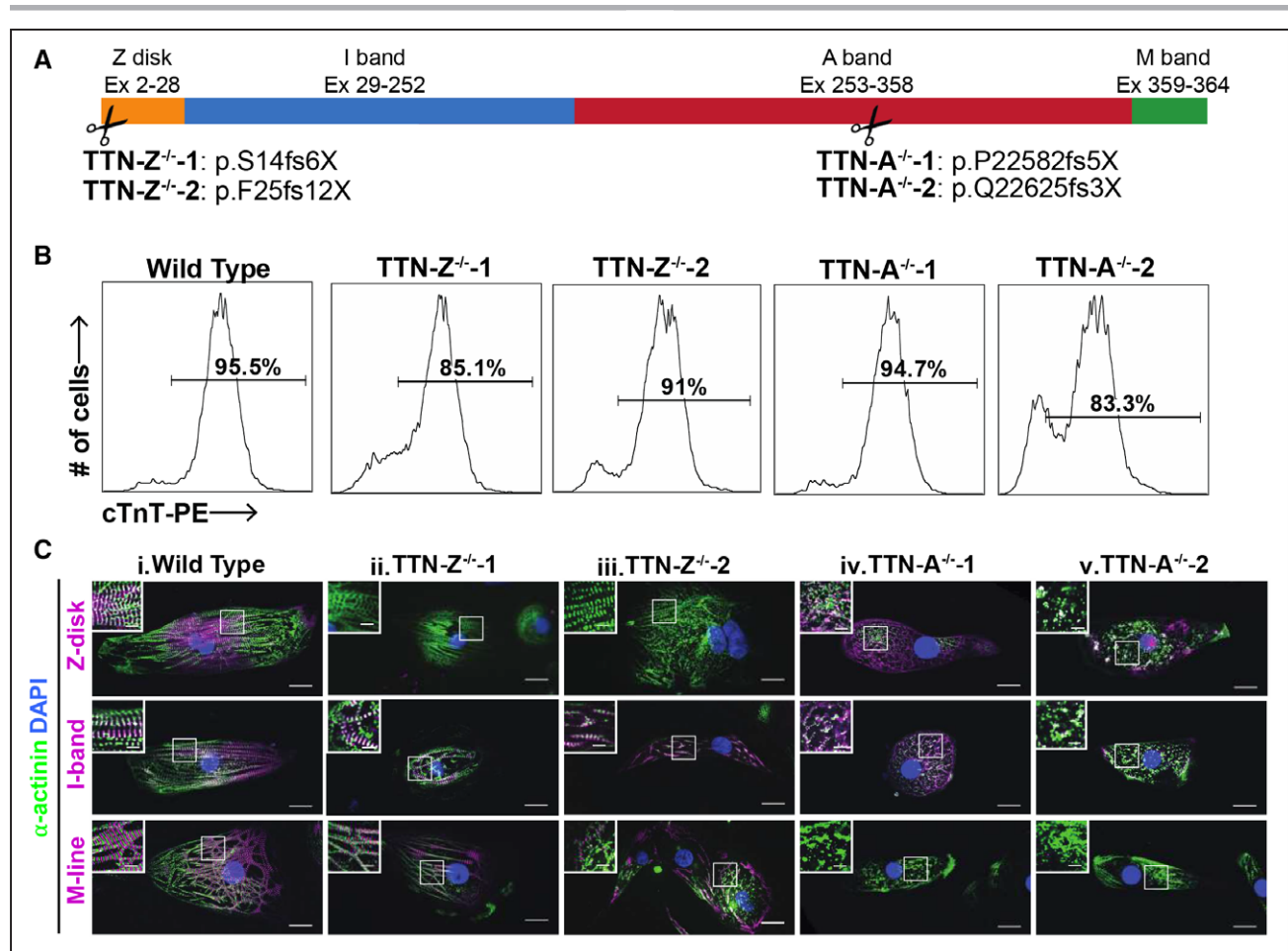


Figure 1. Mutant cell line overview.

A, Exons of the *TTN* gene that encode for each domain of titin and the locations along the titin meta-protein of homozygous mutations specifically engineered into human induced pluripotent stem cell (hiPSC) lines. **B**, Representative cardiac troponin T (cTnT) flow cytometry results of 30- to 31-day-old hiPSC-cardiomyocytes (hiPSC-CMs) show that all cell lines can differentiate into high-purity populations of cardiomyocytes. **C**, Immunohistochemistry of hiPSC-CMs from each cell line using titin antibodies that recognize the Z disk, distal I-band, and M-line regions of the protein. Column i shows that wild-type (WT) CMs stain positively for all titin epitopes and show sarcomere formation. Columns ii and iii show that *TTN-Z*^{-/-} CMs have sarcomere formation but stain positively for titin domains only downstream of the Cronos start site. In columns iv and v, *TTN-A*^{-/-} CMs stain positively for N-terminal antibodies and do not form sarcomeres. In each panel, large image: scale bar=20 μm; inset image: scale bar=5 μm. White boxes indicate regions magnified in the inset image. Ex indicates exon; and PE, phycoerythrin.

(Figure 1B). Given that we had hypothesized that none of the mutant cell lines would develop sarcomeres, we were surprised to find that the *TTN-Z*^{-/-} lines, which cause the most proximal truncation, formed monolayers of beating CMs. The *TTN-A*^{-/-} lines did not visibly contract, even in populations that had a high percentage of cardiac troponin T-positive cells.

Because *TTN-Z*^{-/-}-CMs visibly contracted, we hypothesized that these cells were expressing some form of titin that allowed them to form functioning sarcomeres. Levels of full-length titin transcript were not significantly different across any of the cell lines, indicating that nonsense-mediated decay of the *TTN* transcript does not occur (Figure IIB in the online-only Data Supplement). To investigate titin expression, we performed immunocytochemistry on hiPSC-CMs with antibodies to probe for the Z disk, distal I-band, and M-line domains of titin (Figure 1C). WT samples stained positively for all 3 titin epitopes, and the antibodies localized within

the sarcomere in the expected patterns. *TTN-Z*^{-/-}-CMs exhibited striated staining with α-actinin, and interestingly, these sarcomeres stained positively only for distal I-band and M-line titin, both of which are downstream of the mutation introduced into this cell line. Finally, *TTN-A*^{-/-}-CMs did not form distinct sarcomeres, and diffuse α-actinin, Z disk, and I-band titin signals were observed. The M-line domain of titin, which is downstream of the mutation in these cells, was not detected. These data indicate that despite inducing a truncating mutation in a constitutively expressed N-terminal exon, the *TTN Z*^{-/-} cells expressed distal elements of *TTN* that supported myofibrillogenesis and contractility.

Titin Z Disk Truncations Are Partially Rescued by Cronos Titin

The expression of distal titin epitopes with Z disk truncation mutations suggested that an alternative transcript

was initiated 3' to our mutations. Zou et al²⁹ recently identified an internal promoter in zebrafish *ttf*, which initiates transcription from a previously unrecognized transcriptional start site located in the distal I-band portion.²⁹ Called Cronos, this C-terminal isoform of titin is predicted to be approximately two-thirds the size of the full-length isoforms and to contain the distal I-band, A-band, and M-line regions, consistent with our epitope maps in the Z disk truncation lines (Figure 2A). Gene targeting approaches disrupting Cronos titin expression in zebrafish cause significant myofibrillar disarray.²⁹ Although the transcript has been detected in mammalian

cardiac samples,²⁹ until now, no studies have identified the Cronos titin protein or investigated its role in human CMs. We hypothesized that the *TTN-Z*^{-/-}-CMs express Cronos titin, which allowed some sarcomere formation in these cells.

To begin investigating this hypothesis, we revisited chromatin immunoprecipitation sequencing data from human embryonic stem cells undergoing cardiac differentiation.³⁵ We identify 2 peaks of H3K4me3 (a promoter-specific epigenetic mark) within *TTN* in definitive CMs 14 days after the start of differentiation that are not present during earlier stages of differen-

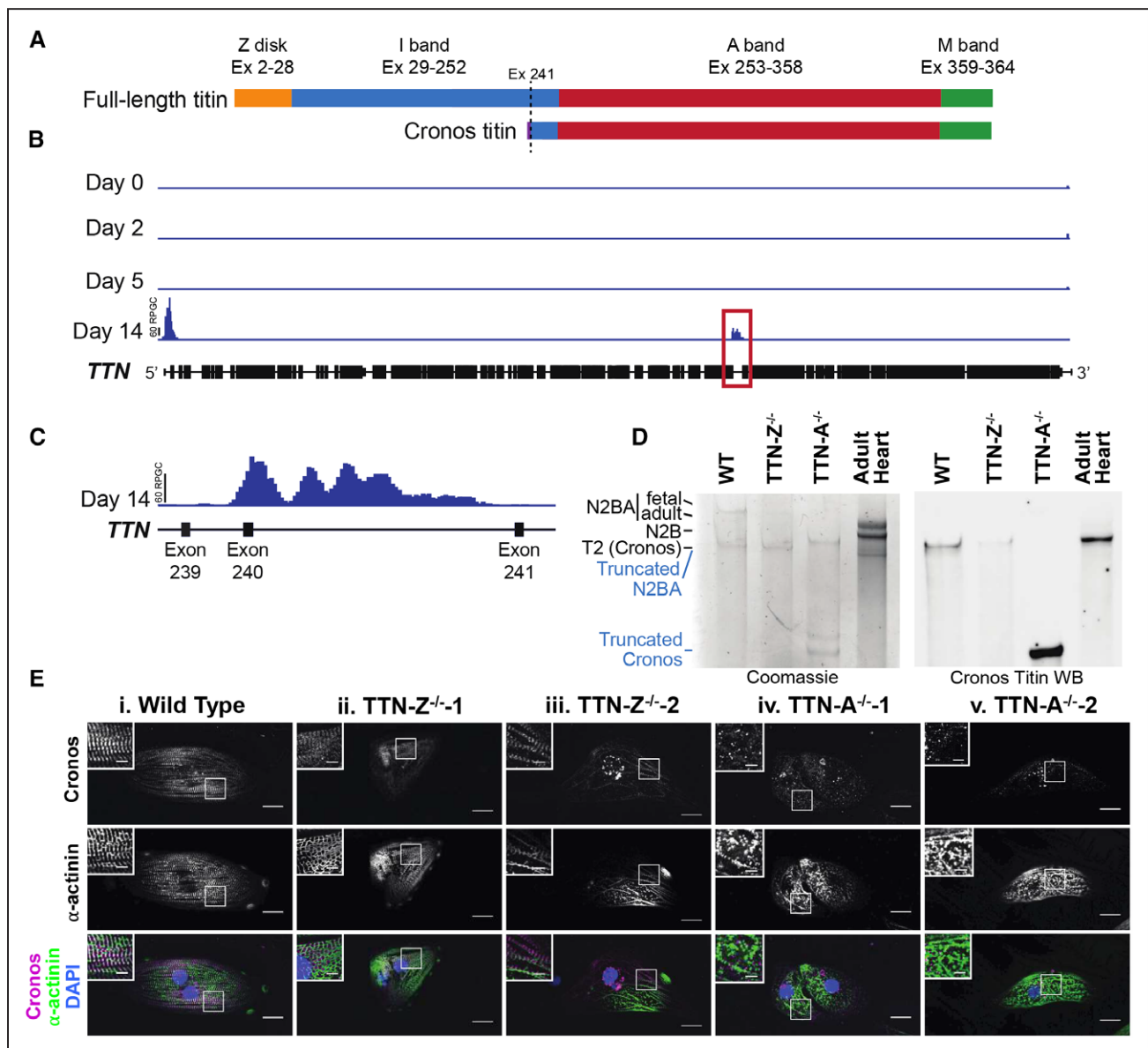


Figure 2. Cronos titin is expressed in human induced pluripotent derived cardiomyocytes (CMs).

A, Schematic of domains expressed in full-length and Cronos titin. Purple indicates a short Cronos-specific region that is intronic to full-length titin. **B**, H3K4me3 enrichment in human embryonic stem CMs during differentiation. **C**, An enlarged view of the region in the red box in **A** indicating a prominent peak near the expected Cronos titin transcription start site between exons 239 and 240. **D**, Coomassie-stained gel and Western blot of protein samples from wild type (WT) and mutant cell lines and adult human heart tissue demonstrate that the Cronos antibody is specific. Blue labels refer to the *TTN-A*^{-/-} lane; black labels refer to all other samples. **E**, Staining for the N-terminal of Cronos titin indicates a doublet pattern around the Z disks in (i) WT and (ii) and (iii) *TTN-Z*^{-/-} CMs and diffuse staining in (iv) and (v) *TTN-A*^{-/-} CMs. In each panel, large image: scale bar=20 μm; inset image: scale bar=5 μm. White boxes indicate regions magnified in inset image. Ex indicates exon.

tiation (Figure 2B). One peak localizes to the 5' end of *TTN* corresponding to the transcriptional start site of full-length titin, and the second prominent peak corresponds to the locus previously proposed for the Cronos titin transcriptional start site in the intron between exons 240 and 241 (Figure 2C). Profiles for the repressive H3K27me3 chromatin mark did not show significant peaks in the *TTN* locus at any time point studied (Figure IIA in the online-only Data Supplement). The appearance of H3K4me3 deposition without H3K27me3 is a pattern typically observed in cardiac structural genes.³¹ Together, these provide genomic evidence to support the presence of an internal Cronos-specific promoter within the *TTN* locus in human stem cell-derived CMs.

To determine whether Cronos titin protein was present in hiPSC-CMs, we performed loose gel electrophoresis to distinguish titin isoforms by molecular weight. Analysis of total protein with a Coomassie stain indicates that both N2BA and T2 titin are present in WT samples but only T2 titin is present in *TTN-Z^{-/-}* cells (Figure 2D). The T2 band has previously been described as a proteolytic degradation product of N2B and N2BA titin,^{36–38} but we and others hypothesized that this band contains the novel isoform Cronos because of its similar expected molecular weight (≈ 2.2 MDa).²⁹ To test this idea, we raised a custom antibody to recognize the N-terminus of Cronos, the first 13 residues of which are specific to this isoform²⁹ (see Methods in the online-only Data Supplement for details). Western blots against hiPSC-CM lysates and human adult left ventricular tissue with this antibody labeled the T2 band but did not detect any of the other titin isoforms present, confirming that this band includes Cronos titin. The Cronos titin band was also recognized by antibodies for the A-band/I-band junction and M-line regions of titin (Figure IIC in the online-only Data Supplement). Several lower-weight titin bands were detected in the *TTN-A^{-/-}*-CMs on the Coomassie-stained gel and Cronos titin Western blot, indicating that only truncated versions of N2BA and Cronos titin are present in these cells. Taken together, these data demonstrate that the T2 band includes Cronos titin, indicate that this novel isoform is expressed in hiPSC-CMs and human heart tissue, and reveal that *TTN-Z^{-/-}* CMs are solely expressing this isoform.

To investigate whether Cronos titin was being integrated into sarcomeres and to establish its localization in the cell lines, we performed immunostaining with our custom antibody (Figure 2E). This revealed doublet patterns surrounding the Z disks in both WT and *TTN-Z^{-/-}* samples, demonstrating that Cronos titin is being expressed and integrated into sarcomeres in these cells. *TTN-A^{-/-}* samples stained diffusely for Cronos titin, similar to the pattern observed with other titin antibodies that recognize regions upstream of the truncating mutation. This pattern is also consistent with Western blot data indicating that the *TTN-A^{-/-}* cells are expressing

a large truncation product of this isoform. Thus, we conclude that the ability of *TTN-Z^{-/-}* mutants to form sarcomeres likely results from the ability of Cronos to substitute, at least in part, for full-length titin.

Force Production in EHTs and Single Cells

After observing that *TTN-Z^{-/-}*-CMs can form sarcomeres and contract with Cronos used as a substitute for full-length titin, we were interested in establishing whether they had contractility comparable to that of WT cells. To investigate force production, we characterized the contractile function of WT and mutant CMs in a multicellular context using EHTs³³ and as single cells.³⁹ Consistent with observations of CMs in monolayers, both WT and *TTN-Z^{-/-}* EHTs visibly contracted, whereas *TTN-A^{-/-}* EHTs did not visibly contract, although they did compact the fibrin gel. Measurements of paced twitches 3 weeks after seeding indicate that *TTN-Z^{-/-}* EHTs produced only $\approx 10\%$ of absolute force produced by WT EHTs (Figure 3A and 3B) and $\approx 25\%$ of active tension compared with WT (Figure 3C). The time to peak WT and *TTN-Z^{-/-}* EHT twitches was slightly decreased, although the maximum rate of force development was dramatically slower (Figure IIIF and IIIG in the online-only Data Supplement). Neither 50% or 90% relaxation time was significantly different in *TTN-Z^{-/-}* EHTs, although passive force was significantly decreased (Figure IIIB, IIID, and IIIE in the online-only Data Supplement). Staining for different regions of titin indicated that titin expression was the same in EHTs as in single cells (Figure IV in the online-only Data Supplement). Taken together, these data indicate that although *TTN-Z^{-/-}*-CMs are able to form sarcomeres and contract, they produce only a small fraction of the force of WT cells in engineered tissues.

To determine whether the weak force production of *TTN-Z^{-/-}* EHTs was caused by attenuated twitches of individual cells, we characterized single-cell contractility using a micropost-based assay system³⁹ (Figure 3D through 3F and Figure V in the online-only Data Supplement). *TTN-Z^{-/-}*-CMs produce significantly lower force both on a whole-cell level and when normalized for cell area (Figure 3D through 3F). Interestingly, maximum twitch velocity, twitch power, cell size, and passive force were not different between cell types, although both upstroke and relaxation times were decreased in *TTN-Z^{-/-}*-CMs compared with controls (Figure 3G and Figure V in the online-only Data Supplement). Notably, the force difference between single WT-CMs and *TTN-Z^{-/-}*-CMs is less dramatic than that observed in the EHT system. This may be partially caused by the younger age and less mature state of cells used in the micropost system, along with the fact that multicellular forces are generated in series in the EHTs, which would be expected to increase the difference between WT and knockout (KO) cells (see Discussion).

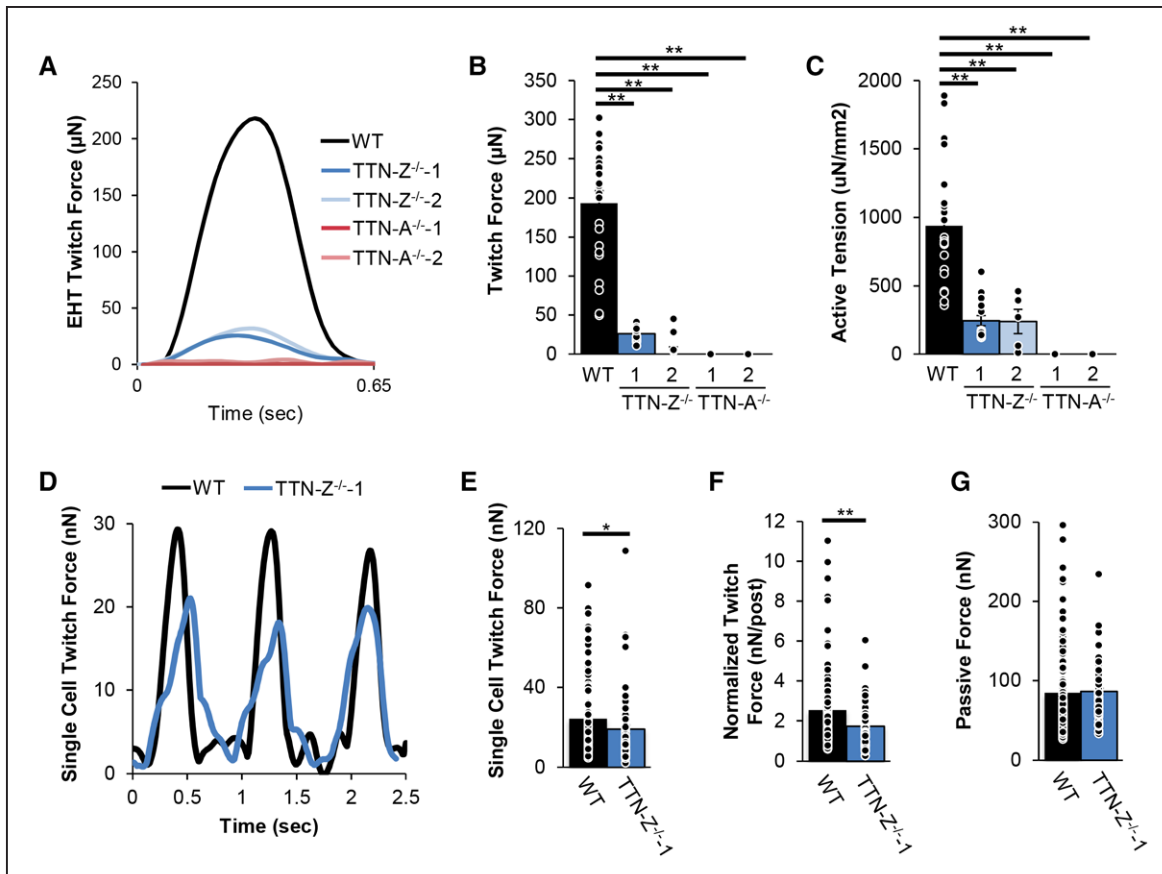


Figure 3. Force mechanics of mutant cell lines.

A, Representative twitches of engineered heart tissues (EHTs) seeded with human induced pluripotent stem cell derived cardiomyocytes show that wild-type (WT) and TTN-Z^{-/-} EHTs produce measurable force, whereas TTN-A^{-/-} EHTs do not. Measurements of EHTs 3 weeks after seeding while paced at 1.5 Hz show that compared with WT, TTN-Z^{-/-} (**B**) average absolute twitch forces and (**C**) active tension normalized to cross-sectional area are significantly reduced. **D**, Sample twitch force traces of single-cell micropost measurements. TTN-Z^{-/-}-CMs produce lower (**E**) whole-cell twitch force and (**F**) twitch force when normalized to cell size. **G**, There was no significant difference in passive force. **B** and **C**, WT: n=23; TTN-Z^{-/-}-1: n=16; TTN-Z^{-/-}-2: n=5; TTN-A^{-/-}-1: n=16; and TTN-A^{-/-}-2: n=17. *P* values were calculated with ANOVAs and follow-up Tukey post hoc tests. Adjusted *P* values were computed with the Benjamini and Hochberg method. **E** through **G**, WT: n=107; TTN-Z^{-/-}-1: n=71. *P* values were calculated with the Student *t* test. Adjusted *P* values were computed with the Benjamini and Hochberg method. Error bars indicate SE. *Adjusted *P*<0.05. **Adjusted *P*<0.01.

To determine whether the reduced force produced by TTN-Z^{-/-}-CMs was caused by differences in calcium handling, we measured Ca²⁺ transients during electric pacing of single cells plated on fibronectin-coated glass slides (Figure VI in the online-only Data Supplement). Interestingly, we found that the magnitude of calcium transients in TTN-Z^{-/-} and TTN-A^{-/-} CMs was not lower than in WT controls, although some calcium release was slightly slower and reuptake was slightly faster in some groups. From these data, we conclude that differences in calcium transients do not explain attenuated force production observed in individual TTN-Z^{-/-}-CMs.

Cell Morphology and Sarcomere Formation

To measure whether sarcomere morphology was distinct between WT and TTN-Z^{-/-}-CMs, we fixed and stained cells after 30 and 60 days of culture on nanopatterned substrates, which provide external

cues to improve elongation and sarcomere alignment.^{40,41} Myofibrils in TTN-Z^{-/-} cells were noticeably sparser compared with WT controls, and maximum myofibril bundle width within each cell was less than half of control at both time points (Figure 4A and 4B). In addition, although WT myofibril bundle width significantly increased between 30 and 60 days cultured on the nanopatterns, indicative of continued hypertrophy and increasing organization, it did not change in TTN-Z^{-/-}-CMs. This could indicate that TTN-Z^{-/-} myofibril bundling or stability is compromised. Interestingly, sarcomere length, circular variance (a measure of sarcomere disarray), cell area, maximum cell width, and cell length were not significantly different between WT and TTN-Z^{-/-}-CMs at either time point (Figure VIIA through VIIC, VIIF, and VIIG in the online-only Data Supplement). In addition, the TTN-Z^{-/-}-CMs exhibited higher multinucleation than WT controls at the 60-day time point. Although overall rates of multinucleation were nonsignificantly higher in TTN-Z^{-/-} cells at

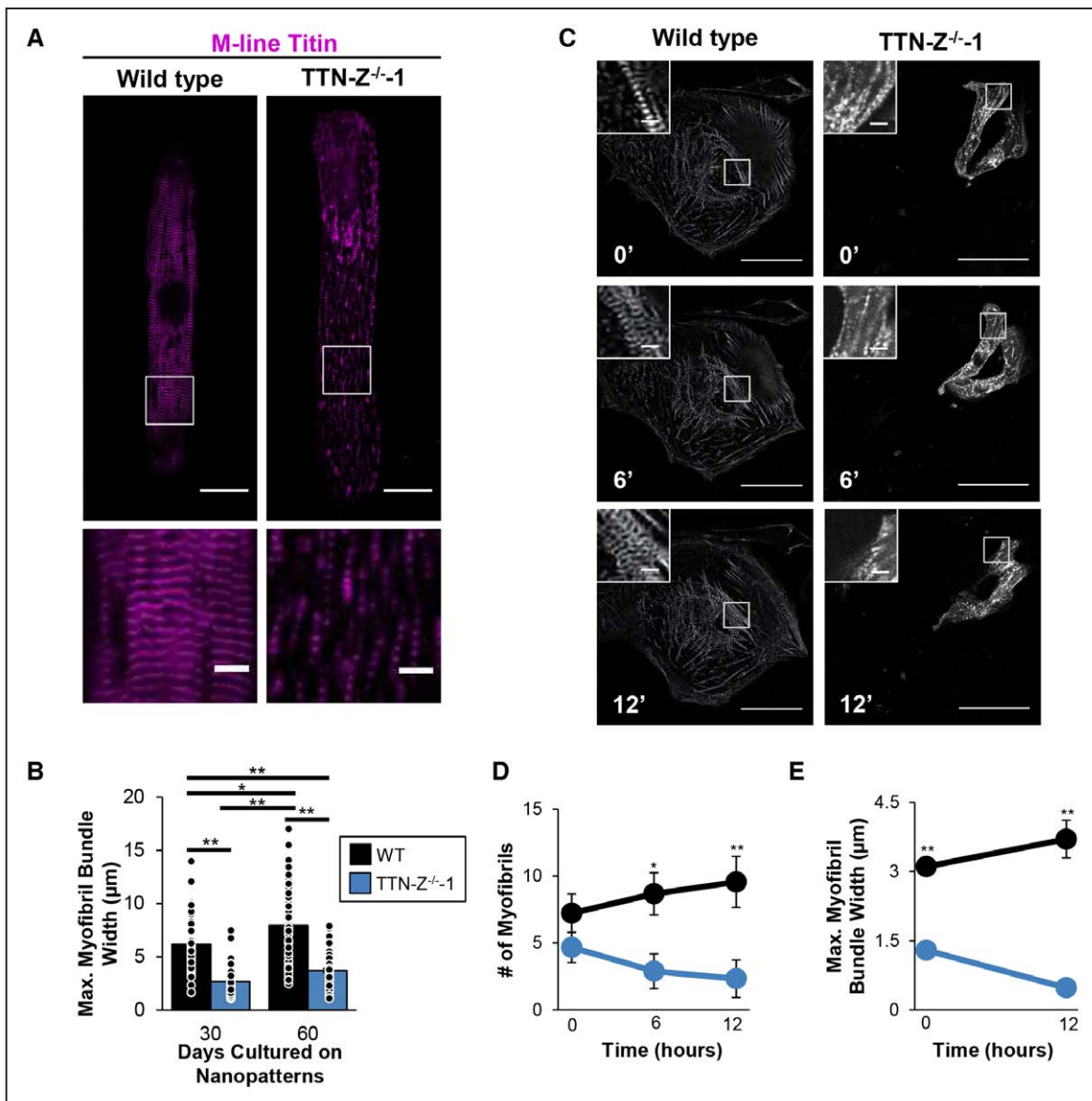


Figure 4. Myofibril morphology in wild-type (WT) and TTN-Z^{-/-} cardiomyocytes (CMs).

A, Representative image of TTN-Z^{-/-}-CMs plated on nanopatterns for 60 days shows significantly smaller myofibrillar bundles compared with wild type (WT). **B**, Morphological analysis of human induced pluripotent stem cell-derived cardiomyocytes (hiPSC-CMs) cultured on nanopatterned surfaces for 30 or 60 days indicates that maximal (Max.) myofibril bundle width was decreased in TTN-Z^{-/-}-CMs compared with WT at both time points. **C**, Time-lapse images of hiPSC-CMs expressing mCherry-tagged α -actinin show that **(D)** WT-CMs consistently build myofibrils whereas TTN-Z^{-/-} CMs have unstable myofibrils and **(E)** WT-CMs increase myofibril bundle width whereas TTN-Z^{-/-} CMs decrease bundle width. Large images: scale bars=50 μ m; inset images: scale bars=5 μ m. In **B**, WT: n=43 to 57; TTN-Z^{-/-}: n=66 to 70. Nominal *P* values were calculated with ANOVAs. Adjusted *P* values were calculated with the Tukey post hoc test and are reported in this figure. In **D** and **E**, WT and TTN-Z^{-/-}: n=9. *P* values were calculated with Student *t* tests. Adjusted *P* values were computed with the Benjamini and Hochberg method. In all panels, error bars indicate SE. *Adjusted *P*<0.05. **Adjusted *P*<0.01.

this time point, there were striking incidences of cells that contained 4 or 5 nuclei (Figure VIID and VIII E in the online-only Data Supplement). This was never observed in the WT samples and may be explained by a nuclear role of full-length titin or a cytoplasmic role in inhibiting nuclear division.^{42–44}

To further investigate sarcomere formation in TTN-Z^{-/-}-CMs, we lentivirally transduced CMs with mCherry-tagged α -actinin, replated the cells, and performed live-cell imaging every 30 minutes for 12 hours. WT CMs exhibited the expected peripheral flow of α -actinin in

stress fiber-like structures at the edge of the cell, which then became centripetal as the α -actinin condensed and formed Z disks near the center of the cell, as previously reported.⁴⁵ During the 12 hours of imaging, a drastic increase in myofibril number and bundle width was observed in WT-CMs (Figure 4C through 4E and Movie I in the online-only Data Supplement). In contrast, TTN-Z^{-/-}-CMs did not show any peripheral flow of α -actinin, and myofibril number and bundle width decreased (Movie II in the online-only Data Supplement). This indicates that TTN-Z^{-/-}-CMs are not able to

properly bundle myofibrils and that the small myofibrils formed are not stable.

Expression of Cronos in Human Fetal and Adult Hearts

Having established Cronos titin expression and integration into sarcomeres in hiPSC-CMs, we wanted to examine whether this isoform was similarly expressed in human tissue. To study the expression levels and localization of Cronos titin in development, we performed immunohistochemistry on human fetal and adult cardiac ventricular samples using our Cronos titin-specific

antibody (Figure 5A). Staining for β -myosin heavy chain revealed clear striations in all samples studied, with increasing density and alignment of myofibrils in older fetal and adult samples. Cronos titin staining was clearly visible throughout the tissue of day 54 and 81 fetal heart samples. As in the hiPSC-CMs, Cronos formed doublets within the sarcomere of fetal hearts, corresponding to the space between the thick filament and the Z disk. Myofibril density and Cronos titin staining were noticeably higher in the day 81 than in the day 54 sample. Interestingly, Cronos titin staining was drastically reduced in the day 130 fetal sample, in which it was barely visible in isolated portions of the

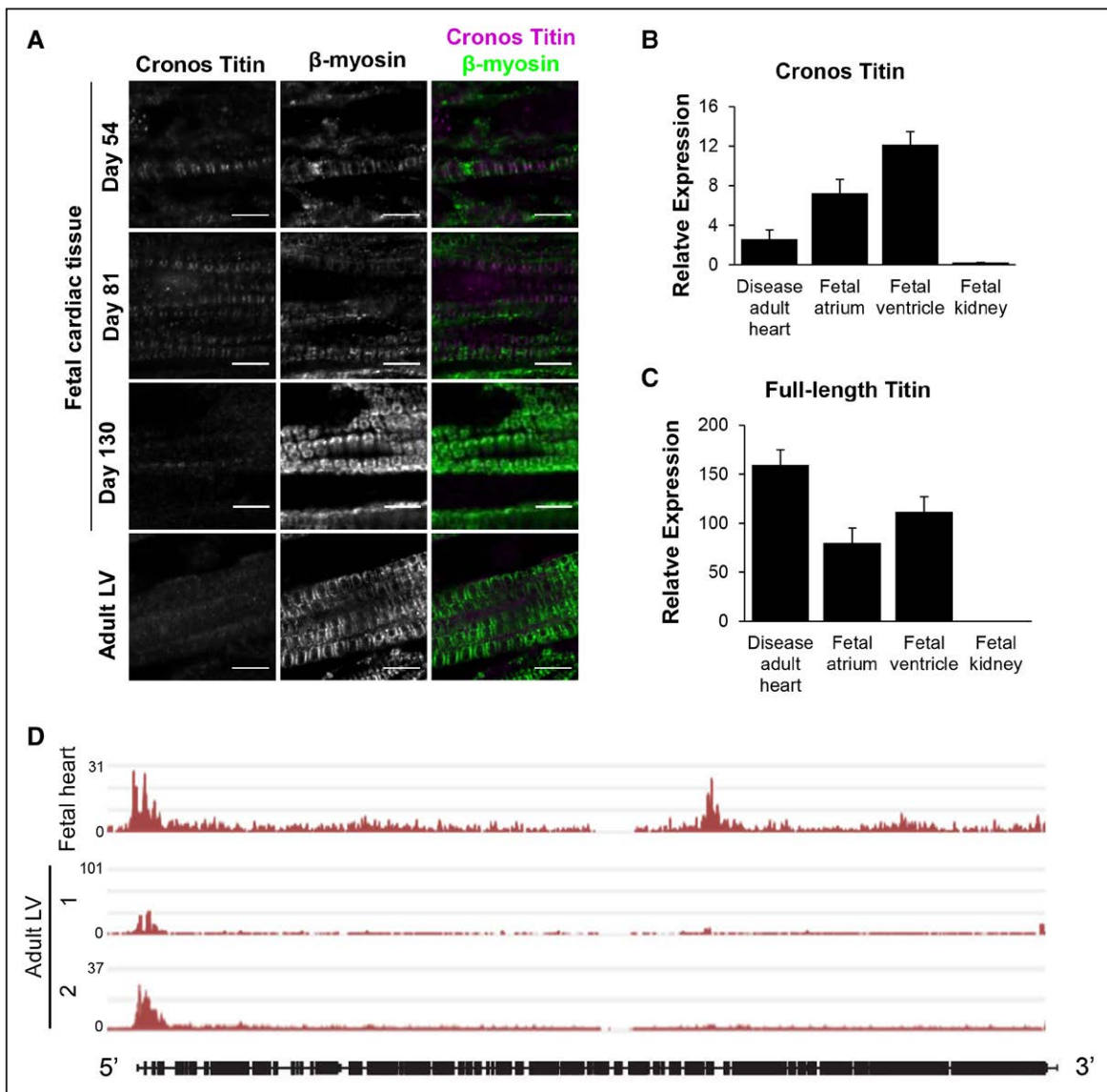


Figure 5. Cronos expression in human cardiac samples.

A, β -Myosin staining shows the presence of myofibrils in all samples. Cronos titin stains strongly in day 54 and 81 fetal samples and indicates localization to the edge of the thick filament. In day 130 samples, Cronos titin is still visible but much sparser and has lost the doublet pattern observed in younger fetal samples. Cronos titin is barely detectable in adult left ventricle (LV) samples. Scale bars=5 μ m. **B**, Cronos titin transcript is expressed in fetal atrium and ventricle samples and adult LV samples but not in fetal kidney. **C**, Full-length titin transcript is expressed in all cardiac samples studied but not fetal kidney. **D**, H3K4me3 marks along *TTN* in fetal whole heart (Gene Expression Omnibus accession No. GSM772735) and adult LV tissue samples (Gene Expression Omnibus accession Nos. GSM910580 and GSE101357) expressed as fold change over baseline. Data are from Dunham et al⁴⁶; details are given in Methods. In **B** and **C**, diseased human heart: n=3; fetal atrium: n=4; fetal ventricle: n=2; and fetal kidney: n=3. Expression calculated relative to hypoxanthine phosphoribosyltransferase with the $\Delta\Delta C_T$ method. Error bars represent SE.

tissue. In sections where Cronos titin was observed, it remained in a striated pattern but had lost the doublet pattern detected in earlier fetal samples. Adult tissue did not show a clear pattern of Cronos titin localization, and the signal was barely above background fluorescence observed in unstained tissue (Figure VIII in the online-only Data Supplement). Cronos and full-length titin transcripts were detected in adult and fetal cardiac samples, and although low sample numbers limit statistical analysis, Cronos appears to be more highly expressed in fetal than in adult tissue (Figure 5B and 5C). In addition, chromatin immunoprecipitation sequencing data indicate that a fetal whole-heart sample has H3K4me3 peaks at both the full-length and Cronos transcription start sites in *TTN*, similar to that observed in hPSC-CM samples, whereas adult LV samples have peaks only at the full-length start site (Figure 5D). These data confirm that Cronos titin is highly expressed in human fetal cardiac tissue.

Cronos Titin Is Necessary for Organized Sarcomere Formation

To investigate the role of Cronos titin in CM function and sarcomere formation, we generated 2 Cronos KO hiPSC lines, both of which expressed full-length titin. Both hiPSC lines differentiated into visibly beating CMs, and immunostaining for Cronos indicated that none was integrated into sarcomeres (Figure 6A), whereas staining showed that domains present in full-length titin were still present and correctly localized relative to α -actinin (Figure IX in the online-only Data Supplement). A Western blot using the custom Cronos titin antibody indicated that this isoform was absent in the Cronos KO-CM (Figure 6B and Figure X in the online-only Data Supplement). EHTs prepared with Cronos KO-CM produce less than half the twitch force (92.6 and 29.1 μN in Cronos KO versus 193.4 μN in WT) and active tension (468.6 and 349.2 $\mu\text{N}/\text{mm}^2$ in Cronos KO versus 939.6 $\mu\text{N}/\text{mm}^2$ in WT) compared with WT and have less than half the

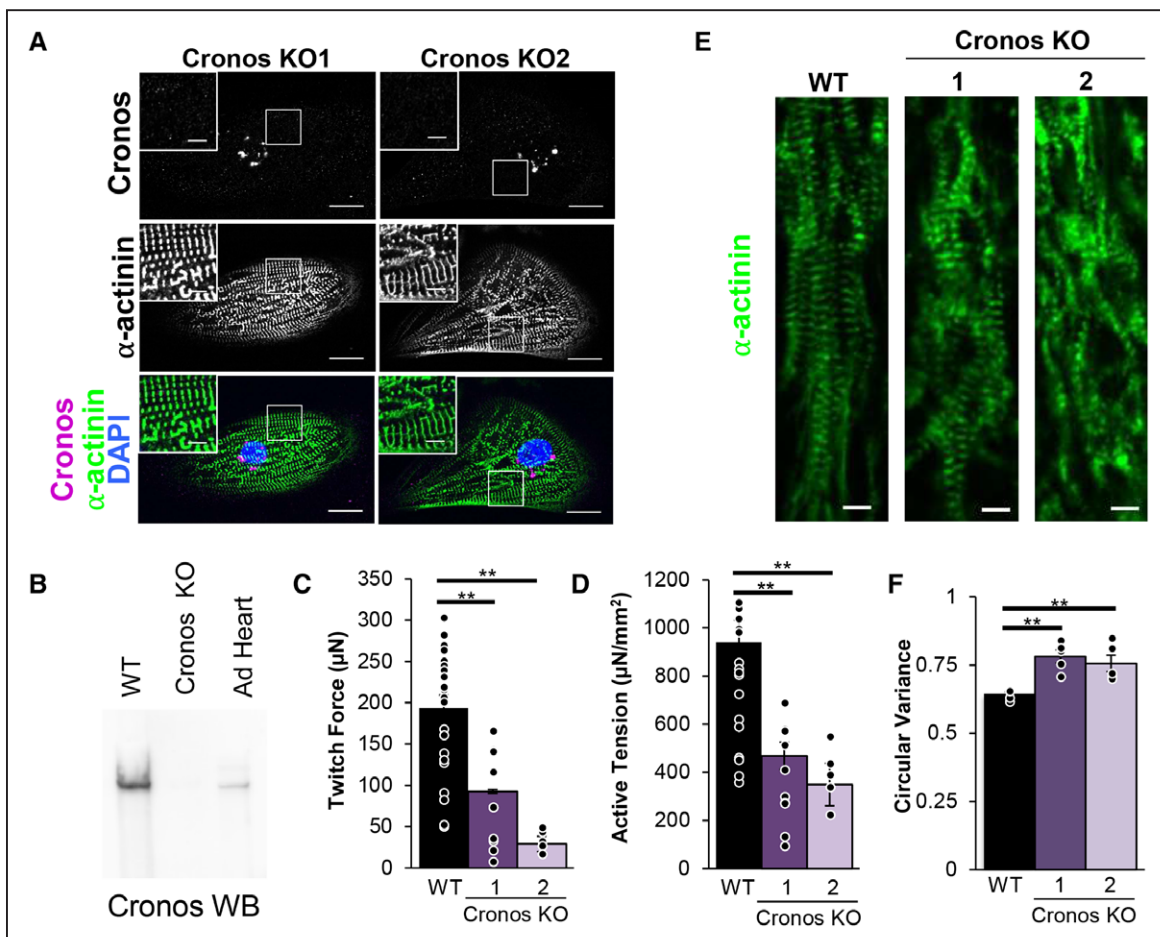


Figure 6. Characterization of Cronos knockout (KO) human induced pluripotent derived cardiomyocytes (CMs).

A, Cronos KO CMs do not stain for Cronos titin but do form sarcomeres. In each panel, large image: scale bar=20 μm ; inset image: scale bar=5 μm . White boxes indicate regions magnified in inset image. Engineered heart tissues (EHTs) seeded with Cronos KO CMs produce lower (**B**) twitch force and (**C**) active tension normalized to cross-sectional area compared with wild-type (WT). **D**, Representative images of EHT immunohistochemistry show myofibrillar disarray in Cronos KO samples, and (**E**) when this is quantified by measuring circular variance, it is found to be statistically significant. **F**, Calcium transient magnitudes of single Cronos KO CMs are not significantly different compared with WT. **B** and **C**, WT: n=23; Cronos KO-1: n=12; and Cronos KO-2: n=6. **E**, WT: n=6; Cronos KO-1: n=5; and Cronos KO-2: n=5. **F**, WT: n=35; Cronos KO-1: n=32; and Cronos KO-2: n=22. Error bars indicate SE. Nominal *P* values were calculated with ANOVAs. Adjusted *P* values were calculated with the Tukey post hoc test and are reported in this figure. Ad indicated adult; and WB, western blot. **Adjusted *P*<0.01.

maximum twitch force velocity (642.7 and 260.4 $\mu\text{m/s}$ in Cronos KO versus 1330.4 $\mu\text{m/s}$ in WT; Figure 6B and 6C and Figure XC and XD in the online-only Data Supplement). Interestingly, passive force and twitch kinetics were not different in Cronos KO compared with WT (Figure XA and XB in the online-only Data Supplement). To elucidate the cause of reduced force development, we performed immunohistochemistry on the WT and Cronos EHTs and measured sarcomere length and circular variance, a measure of myofibril alignment. Although sarcomere length was no different between the groups, the myofibrils of the Cronos KO EHTs had significantly more disarray compared with WT (Figure 6D and 6E). In addition, single-cell measurements indicated that there was no significant difference in the magnitude of calcium transients, although the maximum rate of calcium release was slower (Figure XI in the online-only Data Supplement). This indicates that the reduced force production in hiPSC-CMs lacking Cronos titin may result from myofibril disarray.

DISCUSSION

To assess the role of titin in the formation of sarcomeres, we generated 2 hiPSC lines with homozygous mutations in constitutively expressed exons of *TTN*. We hypothesized that proximal truncations (*TTN-Z^{-/-}*) would produce more severe phenotypes than distal truncations (*TTN-A^{-/-}*). Instead, we found that the proximal truncation mutations were compatible with myofibril assembly and contraction, whereas the distal truncations had neither myofibrils nor contractility. Using a custom-generated antibody, we determined that *TTN-Z^{-/-}*-CMs express the Cronos titin isoform, which appears to initiate transcription from an internal promoter distal to the truncation and is sufficient to support some sarcomere formation. In contrast, *TTN-A^{-/-}* CMs express what are likely truncations of both full-length and Cronos titin and do not form myofibrils, as has been previously reported.²⁶ This study also reported that hiPSC-CMs carrying a homozygous truncation in the early I-band region of titin can form sarcomeres. However, this mutation was in an exon that is only sometimes spliced in, and the sarcomere formation was associated with splicing out the mutated exon.²⁶ In the present study, the engineered Z disk mutations are in a constitutively expressed exon, ruling out variable splicing as a mechanism of escape. Thus, we conclude that Cronos titin is sufficient for some sarcomere formation and that the absence of both full-length and Cronos titin inhibits sarcomerogenesis. Although a dominant-negative effect of the large N-terminal fragments in *TTN-A^{-/-}*-CMs cannot be ruled out from our data, experiments in zebrafish using a combined CRISPR/Cas9 knockout and morpholino knockdown implicate a deficiency of titin rather than a dominant-negative effect.²⁹ In addition,

alternative splicing or other internal start sites in titin could not have been detected by the methods in this study and will require follow-up experiments to assess in this system.

Our data are consistent with a structural role for titin, in particular the C-terminal regions, in sarcomere formation. Signaling roles cannot be ruled out, however, given that titin has multiple functions. For example, it is possible that the absence of the M-line region of titin disrupts signaling pathways dependent on the titin kinase domain, which is involved in protein turnover and hypertrophy.¹⁴ However, several pieces of evidence suggest that this is not the case. Previously, a mouse embryonic stem cell line with a homozygous truncating mutation in the M-line region of titin preventing expression of both the kinase domain and C-terminus of the protein was found to lack sarcomeres when differentiated into CMs.⁴⁷ However, a mouse model harboring a mutation that deletes the kinase domain but not the C-terminal of the protein was observed to form sarcomeres early in embryonic development.⁴⁸ This indicates that it may be the anchoring function of the carboxy terminus of titin, rather than the kinase function, that is required for sarcomere formation. This notion is consistent with our finding that cardiac troponin T and α -actinin protein are both diffusely present in *TTN-A^{-/-}*-CMs and indicates that sarcomeric proteins may still be expressed but cannot assemble into functional units. This suggests that signaling pathways relying on M-line titin may not be crucial for sarcomeric protein expression, whereas other functions of this domain such as anchoring to myomesin may be important for this stage of development.

TTN-Z^{-/-}-CMs produced lower force as both multicellular EHTs and single cells compared with WT CMs, although calcium transients had similar magnitudes. Interestingly, the force deficit of individual cells was not as dramatic as in EHTs. One potential explanation for this could be the greater maturity of the CMs in EHTs compared with monolayers,⁴⁹ such that differences in the rate and extent of myofibril formation and bundling in cells become more pronounced. Another possibility is that the summation of cellular forces in series in tissue compared with single-cell assays is compounding differences in force production or that there is more compliance between coupled cells in *TTN-Z^{-/-}*-EHTs compared with WT.

Staining of human tissue indicated that Cronos titin is most highly expressed in early fetal cardiac tissue, suggesting that it is predominantly a developmental isoform. The T2 band, which we demonstrate includes Cronos titin, has been shown to consistently decrease in intensity in cardiac samples as animals mature³⁶ and as hiPSC-CMs are aged in culture,²⁶ supporting the notion that Cronos titin is predominantly a developmental isoform. Because hiPSC-CMs mature more rapidly in

three-dimensional culture compared with two-dimensional culture,⁵⁰ cells in the EHTs may be more mature and thus express more full-length titin, whereas single cells on microposts are younger and thus may be expressing mostly Cronos titin.

The passive tension measured in individual TTN-Z^{-/-}-CMs was not significantly different compared with WT cells (Figure 5D). This could be explained by the immaturity of the contractile lattice in these cells; fetal cardiac tissue has very low passive tension, especially from titin contributions.^{36,51,52} Our recent studies have indicated that hiPSC-CMs matured for 80 to 100 days on patterned substrates have contractile properties similar to those of 74-day fetal tissue,⁴¹ and because the cells used in the micropost assay were significantly younger than this (35–40 days after differentiation), it is likely that they were less mature. Thus, it is possible that the passive tension being measured from single-cell hiPSC-CMs on the microposts results predominantly from other sources such as nonmuscle actin filaments or intermediate filaments within the cells.⁶

Morphological analysis of the myofibrils indicated that TTN-Z^{-/-} had smaller myofibril bundle widths at the Z disk compared with WT (Figure 4B), suggesting either smaller diameters of individual myofibrils or fewer myofibrils in parallel. Previously, conflicting data have been reported on the necessity of N-terminal titin for the formation of Z disks,^{2,53} and the present study indicates that Z disks are able to form in the absence of the N-terminus of titin. However, the live-cell images of cells expressing tagged α -actinin indicate that the stability or bundling ability of these Z disks is compromised, and they quickly degrade after they are formed. We found that sarcomere length was not significantly different between WT and TTN-Z^{-/-}-CMs, which could indicate that full-length titin is not a major contributor to determining sarcomere length in cells at this stage of maturation. Supporting this notion, the length of I-band titin, which is missing in TTN-Z^{-/-}-CMs, does not influence thin filament length, even in adult mice.⁵⁴

For the first time in human cells, we have knocked out Cronos titin. The resulting CMs exhibit reduced force production and sarcomeric disarray, similar to what was observed in zebrafish.²⁹ Cronos is highly expressed in fetal cardiac tissue samples and appears to have a role in sarcomere formation or stability, particularly in the thick filament, given its likely interaction through the included A-band domains. Although further experiments are necessary to understand the role of this isoform in normal human development, these findings indicate that Cronos is an important player in sarcomerogenesis.

It is striking that CMs are able to form sarcomeres in the absence of full-length titin in TTN-Z^{-/-}-CMs, given that these mutations are not compatible with survival in rodent models.^{16,17} We conclude that sarcomeres

form in TTN-Z^{-/-}-CMs and not TTN-A^{-/-}-CMs because of the presence of Cronos titin, an isoform of titin that we demonstrate for the first time is expressed and integrated into myofibrils of human CMs. According to the findings of this study, it is likely that Cronos is a developmental isoform of titin. We conclude that Cronos titin is necessary for normal sarcomere development and function because full Cronos KO CMs produce lower contractile force and disarrayed sarcomeres. The discovery of this isoform in human samples motivates a closer look at how DCM is caused by truncating mutations in *TTN* and the potential role of Cronos in DCM pathogenesis. In particular, the presence of Cronos titin should be taken into account in the evaluation of hiPSC models of DCM because this isoform clearly plays a significant role in hiPSC-CM function. Elucidating the functions of Cronos titin in human development and DCM will be crucial for fully understanding heart development and disease.

ARTICLE INFORMATION

Received January 8, 2019; accepted August 27, 2019.

The online-only Data Supplement is available with this article at <https://www.ahajournals.org/doi/suppl/10.1161/circulationaha.119.039521>.

Correspondence

Charles E. Murry, MD, PhD, University of Washington, 850 Republican St, Brotman Bldg Room 453, Seattle, WA 98109; or Michael Regnier, PhD, University of Washington, 850 Republican St, South Bldg Room 184, Seattle, WA 98109. Email murry@uw.edu or mregnier@uw.edu

Affiliations

Department of Bioengineering (R.J.Z., J.M., D.-H.K., M.R., C.E.M.), Department of Mechanical Engineering (K.B., A.L., N.J.S.), Department of Pathology (P.A.F., L.P., H.R., X.Y., C.E.M.), Center for Cardiovascular Biology (R.J.Z., A.N.A., K.B., A.L., P.A.F., L.P., H.R., X.Y., J.M., D.-H.K., N.J.S., M.R., C.E.M.), Institute for Stem Cell and Regenerative Medicine (R.J.Z., A.N.A., K.B., A.L., P.A.F., L.P., H.R., X.Y., J.M., D.-H.K., N.J.S., M.R., C.E.M.), and Department of Medicine/Cardiology (C.E.M.), University of Washington, Seattle. Institute of Physiology II, University of Muenster, Germany (M.v.F.-S., W.A.L.). Deutsches Zentrum für Herz-Kreislaufforschung, Partner Site Goettingen, Germany (W.A.L.).

Acknowledgments

The authors thank Dr Bruce Conklin (Gladstone Institute) for providing the WTC11 hiPSC line and Dr Siegfried Labeit (University of Heidelberg) for providing titin antibodies. This research was supported by the Cell Analysis Facility Flow Cytometry and Imaging Core in the Department of Immunology at the University of Washington. They also acknowledge the Mike and Lynn Garvey Cell Imaging Lab at the Institute for Stem Cells and Regenerative Medicine (University of Washington) and its director, Dr Dale Hailey, for assistance with sample imaging and analysis. They thank the Birth Defects Research Laboratory at the University of Washington and its director, Dr Ian Glass, for providing the fetal tissue used in this study. R.J.Z., L.P., H.R., M.R., and C.E.M. conceived experiments. R.J.Z., A.N.A., K.B., A.L., and M.v.F.-S. performed experiments. P.A.F. and J.M. provided experimental support. R.J.Z., L.P., H.R., X.Y., W.A.L., M.R., and C.E.M. interpreted data. D.-H.K. and N.J.S. supervised experimental work. R.J.Z., M.R., and C.E.M. prepared the manuscript.

Sources of Funding

This work was supported by National Institutes of Health grants T32 EB1650 (Dr Zaunbrecher and K. Beussman), F32 HL126332 (Dr Leonard), T32 HL007312 (Dr Fields), R01 HL135143 and R01HL146436 (Dr Kim), R01 HL111197 and R01

HD048895 (Dr Regnier), and R01 HL128362, P01 HL094374, R01 HL084642, U54 DK107979, and P01 GM081619 (Dr Murry); National Science Foundation CBET-1509106 (Dr Sniadecki); German Research Foundation grant SFB1002/TPA08 (W.A.L.); Foundation Leducq Transatlantic Network of Excellence Award (Dr Murry), and a gift from the Robert B. McMillen Foundation (Dr Murry). The Birth Defects Research Laboratory is supported by National Institutes of Health grant R24HD000836 to Dr Ian A. Glass.

Disclosures

Dr Murry is a scientific founder of and equity holder in Cytocardia. Dr Kim is a scientific founder of and equity holder in NanoSurface Biomedical Inc. The other authors report no conflicts.

REFERENCES

- Fürst DO, Osborn M, Nave R, Weber K. The organization of titin filaments in the half-sarcomere revealed by monoclonal antibodies in immunoelectron microscopy: a map of ten nonrepetitive epitopes starting at the Z line extends close to the M line. *J Cell Biol*. 1988;106:1563–1572. doi: 10.1083/jcb.106.5.1563
- Gregorio CC, Trombitás K, Centner T, Kolmerer B, Stier G, Kunke K, Suzuki K, Obermayr F, Herrmann B, Granzier H, et al. The NH2 terminus of titin spans the Z-disc: its interaction with a novel 19-kD ligand (T-cap) is required for sarcomeric integrity. *J Cell Biol*. 1998;143:1013–1027. doi: 10.1083/jcb.143.4.1013
- Young P, Ferguson C, Bañuelos S, Gautel M. Molecular structure of the sarcomeric Z-disk: two types of titin interactions lead to an asymmetrical sorting of alpha-actinin. *EMBO J*. 1998;17:1614–1624. doi: 10.1093/emboj/17.6.1614
- Witt CC, Burkart C, Labeit D, McNabb M, Wu Y, Granzier H, Labeit S. Nebulin regulates thin filament length, contractility, and Z-disk structure in vivo. *EMBO J*. 2006;25:3843–3855. doi: 10.1038/sj.emboj.7601242
- Labeit S, Lahmers S, Burkart C, Fong C, McNabb M, Witt S, Witt C, Labeit D, Granzier H. Expression of distinct classes of titin isoforms in striated and smooth muscles by alternative splicing, and their conserved interaction with filamins. *J Mol Biol*. 2006;362:664–681. doi: 10.1016/j.jmb.2006.07.077
- Granzier HL, Irving TC. Passive tension in cardiac muscle: contribution of collagen, titin, microtubules, and intermediate filaments. *Biophys J*. 1995;68:1027–1044. doi: 10.1016/S0006-3495(95)80278-X
- Linke WA, Popov VI, Pollack GH. Passive and active tension in single cardiac myofibrils. *Biophys J*. 1994;67:782–792. doi: 10.1016/S0006-3495(94)80538-7
- Whiting A, Wardale J, Trinick J. Does titin regulate the length of muscle thick filaments? *J Mol Biol*. 1989;205:263–268. doi: 10.1016/0022-2836(89)90381-1
- Müller S, Lange S, Gautel M, Wilmanns M. Rigid conformation of an immunoglobulin domain tandem repeat in the A-band of the elastic muscle protein titin. *J Mol Biol*. 2007;371:469–480. doi: 10.1016/j.jmb.2007.05.055
- Bennett PM, Gautel M. Titin domain patterns correlate with the axial disposition of myosin at the end of the thick filament. *J Mol Biol*. 1996;259:896–903. doi: 10.1006/jmbi.1996.0367
- Tskhovrebova L, Bennett P, Gautel M, Trinick J. Titin ruler hypothesis not refuted. *Proc Natl Acad Sci USA*. 2015;112:E1172. doi: 10.1073/pnas.1422326112
- Granzier HL, Hutchinson KR, Tonino P, Methawasin M, Li FW, Slater RE, Bull MM, Saripalli C, Pappas CT, Gregorio CC, et al. Deleting titin's I-band/A-band junction reveals critical roles for titin in biomechanical sensing and cardiac function. *Proc Natl Acad Sci USA*. 2014;111:14589–14594. doi: 10.1073/pnas.1411493111
- Obermann WM, Gautel M, Weber K, Fürst DO. Molecular structure of the sarcomeric M band: mapping of titin and myosin binding domains in myomesin and the identification of a potential regulatory phosphorylation site in myomesin. *EMBO J*. 1997;16:211–220. doi: 10.1093/emboj/16.2.211
- Lange S, Xiang F, Yakovenko A, Vihola A, Hackman P, Rostkova E, Kristensen J, Brandmeier B, Franzen G, Hedberg B, et al. The kinase domain of titin controls muscle gene expression and protein turnover. *Science*. 2005;308:1599–1603. doi: 10.1126/science.1110463
- Person V, Kostin S, Suzuki K, Labeit S, Schaper J. Antisense oligonucleotide experiments elucidate the essential role of titin in sarcomerogenesis in adult rat cardiomyocytes in long-term culture. *J Cell Sci*. 2000;113(pt 21):3851–3859.
- Gramlich M, Michely B, Krohne C, Heuser A, Erdmann B, Klaassen S, Hudson B, Magarin M, Kirchner F, Todiras M, et al. Stress-induced dilated cardiomyopathy in a knock-in mouse model mimicking human titin-based disease. *J Mol Cell Cardiol*. 2009;47:352–358. doi: 10.1016/j.jmcc.2009.04.014
- Schafer S, de Marvao A, Adami E, Fiedler LR, Ng B, Khin E, Rackham OJ, van Heesch S, Pua CJ, Kui M, et al. Titin-truncating variants affect heart function in disease cohorts and the general population. *Nat Genet*. 2017;49:46–53. doi: 10.1038/ng.3719
- Akinrinade O, Alastalo TP, Koskenvuo JW. Relevance of truncating titin mutations in dilated cardiomyopathy. *Clin Genet*. 2016;90:49–54. doi: 10.1111/cge.12741
- Norton N, Li D, Rampersaud E, Morales A, Martin ER, Zuchner S, Guo S, Gonzalez M, Hedges DJ, Robertson PD, et al; National Heart, Lung, and Blood Institute GO Exome Sequencing Project and the Exome Sequencing Project Family Studies Project Team. Exome sequencing and genome-wide linkage analysis in 17 families illustrate the complex contribution of TTN truncating variants to dilated cardiomyopathy. *Circ Cardiovasc Genet*. 2013;6:144–153. doi: 10.1161/CIRCGENETICS.111.000062
- Pugh TJ, Kelly MA, Gowrisankar S, Hynes E, Seidman MA, Baxter SM, Bowser M, Harrison B, Aaron D, Mahanta LM, et al. The landscape of genetic variation in dilated cardiomyopathy as surveyed by clinical DNA sequencing. *Genet Med*. 2014;16:601–608. doi: 10.1038/gim.2013.204
- van Spaendonck-Zwarts KY, Posafalvi A, van den Berg MP, Hilfiker-Kleiner D, Bollen IA, Sliwa K, Alders M, Almomani R, van Langen IM, van der Meer P, et al. Titin gene mutations are common in families with both peripartum cardiomyopathy and dilated cardiomyopathy. *Eur Heart J*. 2014;35:2165–2173. doi: 10.1093/eurheartj/ehu050
- Haas J, Frese KS, Peil B, Kloos W, Keller A, Nietsch R, Feng Z, Müller S, Kayvanpour E, Vogel B, et al. Atlas of the clinical genetics of human dilated cardiomyopathy. *Eur Heart J*. 2015;36:1123–1135a. doi: 10.1093/eurheartj/ehu301
- Herman DS, Lam L, Taylor MR, Wang L, Teekakirikul P, Christodoulou D, Conner L, DePalma SR, McDonough B, Sparks E, et al. Truncations of titin causing dilated cardiomyopathy. *N Engl J Med*. 2012;366:619–628. doi: 10.1056/NEJMoa1110186
- Roberts AM, Ware JS, Herman DS, Schafer S, Baksi J, Bick AG, Buchan RJ, Walsh R, John S, Wilkinson S, et al. Integrated allelic, transcriptional, and phenomic dissection of the cardiac effects of titin truncations in health and disease. *Sci Transl Med*. 2015;7:270ra6. doi: 10.1126/scitranslmed.3010134
- Ware JS, Li J, Mazaika E, Yasso CM, DeSouza T, Cappola TP, Tsai EJ, Hilfiker-Kleiner D, Kamiya CA, Mazzarotto F, et al; IMAC-2 and IPAC Investigators. Shared genetic predisposition in peripartum and dilated cardiomyopathies. *N Engl J Med*. 2016;374:233–241. doi: 10.1056/NEJMoa1505517
- Hinson JT, Chopra A, Nafissi N, Polacheck WJ, Benson CC, Swist S, Gorham J, Yang L, Schafer S, Sheng CC, et al. Heart disease: titin mutations in iPSC cells define sarcomere insufficiency as a cause of dilated cardiomyopathy. *Science*. 2015;349:982–986. doi: 10.1126/science.aaa5458
- Schick R, Mekies LN, Shemer Y, Eisen B, Hallas T, Ben Jehuda R, Ben-Ari M, Szantai A, Willi L, Shulman R, et al. Functional abnormalities in induced pluripotent stem cell-derived cardiomyocytes generated from titin-mutated patients with dilated cardiomyopathy. *PLoS One*. 2018;13:e0205719. doi: 10.1371/journal.pone.0205719
- Gramlich M, Pane LS, Zhou Q, Chen Z, Murgia M, Schötterl S, Goedel A, Metzger K, Brade T, Parrotta E, et al. Antisense-mediated exon skipping: a therapeutic strategy for titin-based dilated cardiomyopathy. *EMBO Mol Med*. 2015;7:562–576. doi: 10.15252/emmm.201505047
- Zou J, Tran D, Baalbaki M, Tang LF, Poon A, Pelonero A, Titus EW, Yuan C, Shi C, Patchava S, et al. An internal promoter underlies the difference in disease severity between N- and C-terminal truncation mutations of Titin in zebrafish. *Elife*. 2015;4:e09406. doi: 10.7554/eLife.09406
- Kent WJ, Sugnet CW, Furey TS, Roskin KM, Pringle TH, Zahler AM, Haussler D. The human genome browser at UCSC. *Genome Res*. 2002;12:996–1006. doi: 10.1101/gr.229102
- Palpant NJ, Pabon L, Friedman CE, Roberts M, Hadland B, Zaubrecher RJ, Bernstein I, Zheng Y, Murry CE. Generating high-purity cardiac and endothelial derivatives from patterned mesoderm using human pluripotent stem cells. *Nat Protoc*. 2017;12:15–31. doi: 10.1038/nprot.2016.153
- Tohyama S, Hattori F, Sano M, Hishiki T, Nagahata Y, Matsuura T, Hashimoto H, Suzuki T, Yamashita H, Satoh Y, et al. Distinct metabolic flow enables large-scale purification of mouse and human pluripotent stem cell-derived cardiomyocytes. *Cell Stem Cell*. 2013;12:127–137. doi: 10.1016/j.stem.2012.09.013

33. Bielawski KS, Leonard A, Bhandari S, Murry CE, Sniadecki NJ. Real-time force and frequency analysis of engineered human heart tissue derived from induced pluripotent stem cells using magnetic sensing. *Tissue Eng Part C Methods*. 2016;22:932–940. doi: 10.1089/ten.TEC.2016.0257
34. Kreitzer FR, Salomonis N, Sheehan A, Huang M, Park JS, Spindler MJ, Lizarraga P, Weiss WA, So PL, Conklin BR. A robust method to derive functional neural crest cells from human pluripotent stem cells. *Am J Stem Cells*. 2013;2:119–131.
35. Paige SL, Thomas S, Stoick-Cooper CL, Wang H, Maves L, Sandstrom R, Pabon L, Reinecke H, Pratt G, Keller G, et al. A temporal chromatin signature in human embryonic stem cells identifies regulators of cardiac development. *Cell*. 2012;151:221–232. doi: 10.1016/j.cell.2012.08.027
36. Opitz CA, Leake MC, Makarenko I, Benes V, Linke WA. Developmentally regulated switching of titin size alters myofibrillar stiffness in the perinatal heart. *Circ Res*. 2004;94:967–975. doi: 10.1161/01.RES.0000124301.48193.E1
37. Opitz CA, Linke WA. Plasticity of cardiac titin/connectin in heart development. *J Muscle Res Cell Motil*. 2005;26:333–342. doi: 10.1007/s10974-005-9040-7
38. Makarenko I, Opitz CA, Leake MC, Neagoe C, Kulke M, Gwathmey JK, del Monte F, Hajjar RJ, Linke WA. Passive stiffness changes caused by upregulation of compliant titin isoforms in human dilated cardiomyopathy hearts. *Circ Res*. 2004;95:708–716. doi: 10.1161/01.RES.0000143901.37063.2f
39. Rodriguez ML, Graham BT, Pabon LM, Han SJ, Murry CE, Sniadecki NJ. Measuring the contractile forces of human induced pluripotent stem cell-derived cardiomyocytes with arrays of microposts. *J Biomech Eng*. 2014;136:051005. doi: 10.1115/1.4027145
40. Carson D, Hnilova M, Yang X, Nemeth CL, Tsui JH, Smith AS, Jiao A, Regnier M, Murry CE, Tamerler C, et al. Nanotopography-induced structural anisotropy and sarcomere development in human cardiomyocytes derived from induced pluripotent stem cells. *ACS Appl Mater Interfaces*. 2016;8:21923–21932. doi: 10.1021/acsami.5b11671
41. Pioner JM, Racca AW, Klaiman JM, Yang KC, Guan X, Pabon L, Muskheli V, Zaunbrecher R, Macadangdang J, Jeong MY, et al. Isolation and mechanical measurements of myofibrils from human induced pluripotent stem cell-derived cardiomyocytes. *Stem Cell Reports*. 2016;6:885–896. doi: 10.1016/j.stemcr.2016.04.006
42. Zastrow MS, Flaherty DB, Benian GM, Wilson KL. Nuclear titin interacts with A- and B-type lamins *in vitro* and *in vivo*. *J Cell Sci*. 2006;119(pt 2):239–249. doi: 10.1242/jcs.02728
43. Qi J, Chi L, Labeit S, Banes AJ. Nuclear localization of the titin Z1Z2r domain and role in regulating cell proliferation. *Am J Physiol Cell Physiol*. 2008;295:C975–C985. doi: 10.1152/ajpcell.90619.2007
44. Machado C, Sunkel CE, Andrew DJ. Human autoantibodies reveal titin as a chromosomal protein. *J Cell Biol*. 1998;141:321–333. doi: 10.1083/jcb.141.2.321
45. Chopra A, Kutys ML, Zhang K, Polacheck WJ, Sheng CC, Luu RJ, Eyckmans J, Hinson JT, Seidman JG, Seidman CE, et al. Force generation via β -cardiac myosin, titin, and α -actinin drives cardiac sarcomere assembly from cell-matrix adhesions. *Dev Cell*. 2018;44:87–96.e5. doi: 10.1016/j.devcel.2017.12.012
46. Dunham I, Kundaje A, Aldred SF, Collins PJ, Davis CA, Doyle F, Epstein CB, Fritze S, Harrow J, Kaul R, et al. An integrated encyclopedia of DNA elements in the human genome. *Nature*. 2012;489:57–74. doi: 10.1038/nature11247
47. Musa H, Meek S, Gautel M, Peddie D, Smith AJ, Peckham M. Targeted homozygous deletion of M-band titin in cardiomyocytes prevents sarcomere formation. *J Cell Sci*. 2006;119(pt 20):4322–4331. doi: 10.1242/jcs.03198
48. Weinert S, Bergmann N, Luo X, Erdmann B, Gotthardt M. M line-deficient titin causes cardiac lethality through impaired maturation of the sarcomere. *J Cell Biol*. 2006;173:559–570. doi: 10.1083/jcb.200601014
49. Tulloch NL, Muskheli V, Razumova MV, Korte FS, Regnier M, Hauch KD, Pabon L, Reinecke H, Murry CE. Growth of engineered human myocardium with mechanical loading and vascular coculture. *Circ Res*. 2011;109:47–59. doi: 10.1161/CIRCRESAHA.110.237206
50. Schwan J, Campbell SG. Prospects for *in vitro* myofilament maturation in stem cell-derived cardiac myocytes. *Biomark Insights*. 2015;10(suppl 1):91–103. doi: 10.4137/BMI.S23912
51. Lahmers S, Wu Y, Call DR, Labeit S, Granzier H. Developmental control of titin isoform expression and passive stiffness in fetal and neonatal myocardium. *Circ Res*. 2004;94:505–513. doi: 10.1161/01.RES.0000115522.52554.86
52. Warren CM, Krzesinski PR, Campbell KS, Moss RL, Greaser ML. Titin isoform changes in rat myocardium during development. *Mech Dev*. 2004;121:1301–1312. doi: 10.1016/j.mod.2004.07.003
53. Bowman AL, Catino DH, Strong JC, Randall WR, Kontogianni-Konstantopoulos A, Bloch RJ. The rho-guanine nucleotide exchange factor domain of obscurin regulates assembly of titin at the Z-disk through interactions with Ran binding protein 9. *Mol Biol Cell*. 2008;19:3782–3792. doi: 10.1091/mbc.e08-03-0237
54. Kolb J, Li F, Methawasin M, Adler M, Escobar YN, Nedrud J, Pappas CT, Harris SP, Granzier H. Thin filament length in the cardiac sarcomere varies with sarcomere length but is independent of titin and nebulin. *J Mol Cell Cardiol*. 2016;97:286–294. doi: 10.1016/j.yjmcc.2016.04.013